

# Thermodynamic properties and phase transitions of Tutton salt $(\text{NH}_4)_2\text{Co}(\text{SO}_4)_2 \cdot 6\text{H}_2\text{O}$ crystals

Ae Ran Lim

Received: 6 June 2011 / Accepted: 3 August 2011 / Published online: 21 August 2011  
© Akadémiai Kiadó, Budapest, Hungary 2011

**Abstract** The thermodynamic properties and phase transitions of Tutton salt  $(\text{NH}_4)_2\text{Co}(\text{SO}_4)_2 \cdot 6\text{H}_2\text{O}$  single crystals were investigated with TG, DSC, and NMR. The first mass loss occurs in the vicinity of 360 K ( $T_d$ ), which is interpreted as the onset of partial thermal decomposition. Phase transitions were found at 384 K =  $T_{C1}$ , 415 K =  $T_{C2}$ , and 443 K =  $T_{C3}$ . The temperature dependence of the spin–lattice relaxation time,  $T_1$ , for the H nuclei undergoes slight changes near  $T_{C1}$  and  $T_{C2}$ . These changes are associated with changes in the geometry of the arrangement of water and five  $\text{SO}_4$  oxygens and with proton hopping or the breaking of hydrogen bonds.

**Keywords** Tutton salts ·  $(\text{NH}_4)_2\text{Co}(\text{SO}_4)_2 \cdot 6\text{H}_2\text{O}$  · Thermodynamic property · Relaxation time · Phase transition

## Introduction

Tutton salts are an isomorphous series of monoclinic crystals with the general formula  $\text{M}_2^{\text{II}}\text{M}^{\text{I}}(\text{SO}_4)_2 \cdot 6\text{H}_2\text{O}$  and contain two octahedral hexahydrate complexes  $[\text{M}^{\text{II}}(\text{H}_2\text{O})_6]^{2+}$  in the crystal unit cell, where  $\text{M}^{\text{II}}$  is a divalent cation (Co, Zn, Fe or an ion of the 3d group) and  $\text{M}^{\text{I}}$  is a monovalent cation (K, Rb, Cs, and  $\text{NH}_4$ ) [1]. Tutton salts have played a significant role in physics and chemistry; considerable attention is currently focused on the development of materials suitable for strong energy absorbed by solar collectors. For domestic heating and hot-water supplies, this

energy might be stored chemically in reversible reactions, thermally in the phase changes, or temperature increases of storage materials [2, 3]. The unit cell dimensions and molecular structures of the crystals of this family are very similar. The structural characteristics of the crystals in this series, including the details of their hydrogen bond networks, have been described by Montgomery and Lingafelter [4].  $(\text{NH}_4)_2\text{Co}(\text{SO}_4)_2 \cdot 6\text{H}_2\text{O}$  is a  $\text{M}_2^{\text{II}}\text{M}^{\text{I}}(\text{SO}_4)_2 \cdot 6\text{H}_2\text{O}$  compound with crystals that have monoclinic structure with space group  $P2_1/a$  and lattice parameters  $a = 9.23 \text{ \AA}$ ,  $b = 12.9 \text{ \AA}$ ,  $c = 6.23 \text{ \AA}$ , and  $\beta = 106.9^\circ$  [5]. The unit cell contains two  $\text{Co}^{2+}$  each surrounded by six water molecules forming an octahedron, as shown in Fig. 1. Six water molecules surround the divalent inversion symmetric ( $C_i$ ) sites. The divalent atoms in the unit cell are located at (0, 0, 0) and (1/2, 1/2, 0), while all other atoms are in general positions.

Infrared spectroscopic studies of the vibrational behavior of matrix-isolated ions in Tutton compounds have recently been reported by Marinova et al. [6–11]. Tutton salt crystals doped with  $\text{Mn}^{2+}$ ,  $\text{VO}^{2+}$ ,  $\text{Cu}^{2+}$ ,  $\text{Co}^{2+}$ , and  $\text{Cr}^{3+}$  have been studied by using electron paramagnetic resonance (EPR) [12–24]. In addition, the spin–lattice relaxation at low temperatures of a series of Tutton salt crystals has been studied with EPR; it was found that the relaxation is governed by two-phonon Raman processes without a noticeable contribution from the reorientations of the  $\text{Cu}(\text{H}_2\text{O})_6$  octahedra [18–21, 25, 26].

The interesting properties of Tutton salts have been studied with many methods in recent years. However, the thermodynamic properties and phase transition temperatures of  $(\text{NH}_4)_2\text{Co}(\text{SO}_4)_2 \cdot 6\text{H}_2\text{O}$  crystals have not previously been reported. Further, some questions about Tutton salts are still open, especially those related to the nature of their structural changes and their thermodynamic

A. R. Lim (✉)  
Department of Science Education, Jeonju University,  
Jeonju 560-759, Korea  
e-mail: aeranlim@hanmail.net; arlim@jj.ac.kr

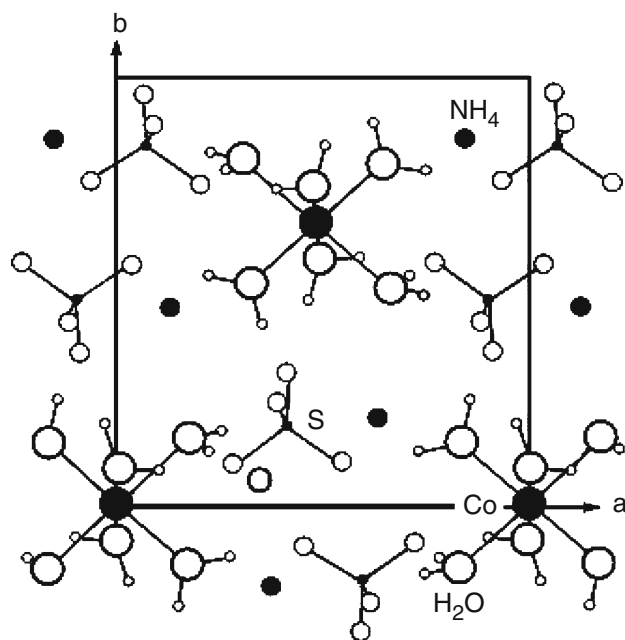


**Fig. 1** Crystal structure of  $(\text{NH}_4)_2\text{Co}(\text{SO}_4)_2 \cdot 6\text{H}_2\text{O}$  projected onto the  $ab$ -plane

properties. In order to obtain detailed information about the dynamics of  $(\text{NH}_4)_2\text{Co}(\text{SO}_4)_2 \cdot 6\text{H}_2\text{O}$  crystals, we measured the nuclear spin–lattice relaxation time,  $T_1$ , of their  $^1\text{H}$  nuclei.

The ammonium and hydrogen bond protons in  $(\text{NH}_4)_2\text{Co}(\text{SO}_4)_2 \cdot 6\text{H}_2\text{O}$  crystals are expected to play a dominant role in their physical properties and phase transition mechanisms. The relationship between the loss of water protons and structural phase transitions is a subject of keen interest. To probe the variations with temperature in the physical properties of  $(\text{NH}_4)_2\text{Co}(\text{SO}_4)_2 \cdot 6\text{H}_2\text{O}$  crystals, the study of the  $^1\text{H}$  spectrum and relaxation times was preferred, because the  $^1\text{H}$  spectrum and relaxation times are likely to be very sensitive to changes in the symmetry of the crystal. In this article, the thermodynamic properties of the crystals, which were determined with thermogravimetry analysis (TG) and differential scanning calorimetry (DSC), are presented. In addition, the temperature dependence of the spin–lattice relaxation time,  $T_1$ , for the  $^1\text{H}$  nuclei in  $(\text{NH}_4)_2\text{Co}(\text{SO}_4)_2 \cdot 6\text{H}_2\text{O}$  crystals was investigated by using a pulse NMR spectrometer. This is the first time that the structural changes of  $(\text{NH}_4)_2\text{Co}(\text{SO}_4)_2 \cdot 6\text{H}_2\text{O}$  crystals have been investigated, and we use these results to analyze the environments of their H nuclei.

## Experimental

$(\text{NH}_4)_2\text{Co}(\text{SO}_4)_2 \cdot 6\text{H}_2\text{O}$  single crystals were grown by using the slow evaporation method from an aqueous solution

containing stoichiometric amounts of  $(\text{NH}_4)_2\text{SO}_4$  and  $\text{CoSO}_4 \cdot 5\text{H}_2\text{O}$ . The prepared samples were approximately  $3 \times 3 \times 2 \text{ mm}^3$  in size. The resulting single crystals were hexagonal and purple.

The NMR results for the  $^1\text{H}$  nuclei in  $(\text{NH}_4)_2\text{Co}(\text{SO}_4)_2 \cdot 6\text{H}_2\text{O}$  single crystals were obtained with the Bruker DSX 200 FT NMR spectrometer at the Korea Basic Science Institute. The static magnetic field was 4.7 T, and the central radio frequency was set at  $\omega_0/2\pi = 200 \text{ MHz}$ . The spin–lattice relaxation time was measured using a saturation recovery pulse sequence,  $\text{sat}-t-\pi/2$ ; the nuclear magnetizations of the  $^1\text{H}$  nuclei at time  $t$  after the  $\text{sat}$  pulse were determined following the  $\pi/2$  excitation pulse. The temperature-dependent NMR measurements were carried out in the range 180–430 K. The sample temperature was maintained at the required constant value by controlling the helium gas flow and the heater current, with an accuracy of  $\pm 0.5 \text{ }^\circ\text{C}$ .

## Experimental results and discussion

The structure of the  $(\text{NH}_4)_2\text{Co}(\text{SO}_4)_2 \cdot 6\text{H}_2\text{O}$  crystals at room temperature was determined using an X-ray diffractometer system (Bruker AXS GMBH) at the Korea Basic Science Institute. The following results were obtained: monoclinic symmetry with cell parameters  $a = 9.256 \text{ \AA}$ ,  $b = 12.819 \text{ \AA}$ ,  $c = 6.361 \text{ \AA}$ , and  $\beta = 107.002^\circ$ . These results are consistent with the data of Montgomery and Lingafelter [27]. In addition, to determine the phase transition temperatures, differential scanning calorimetry (DSC) was carried out on the crystals with a DuPont 2010 DSC instrument. The measurements were performed at a heating rate of  $10 \text{ }^\circ\text{C}/\text{min}$ . Four endothermic peaks were observed, at 384, 415, 443, and 538 K (see Fig. 2). Thermogravimetry analysis (TGA) was then used to determine whether these high-temperature transformations are structural phase transitions or chemical reactions. The thermogram of  $(\text{NH}_4)_2\text{Co}(\text{SO}_4)_2 \cdot 6\text{H}_2\text{O}$  is shown in Fig. 3. The first mass loss begins in the vicinity of 360 K and reaches 14% at 411 K. Above 426 K, thermal decomposition enters a new stage and the residue of final products reaches a value of 72.36% accompanied by the escape of  $\text{H}_2\text{O}$ . Optical polarizing microscopy shows that the crystals are purple at room temperature, and that their color varies with increasing temperature to light pink. This color change might be related to the loss of  $\text{H}_2\text{O}$ . The bulk mass of  $(\text{NH}_4)_2\text{Co}(\text{SO}_4)_2 \cdot 6\text{H}_2\text{O}$  decreases at 360 K ( $T_d$ ), which is interpreted as the onset of partial thermal decomposition, and reaches complete thermal decomposition into  $(\text{NH}_4)_2\text{Co}(\text{SO}_4)_2$  around 495 K. The DSC, TG, and optical polarizing microscopy results for  $(\text{NH}_4)_2\text{Co}(\text{SO}_4)_2 \cdot 6\text{H}_2\text{O}$  crystals show that the mass loss in the vicinity of

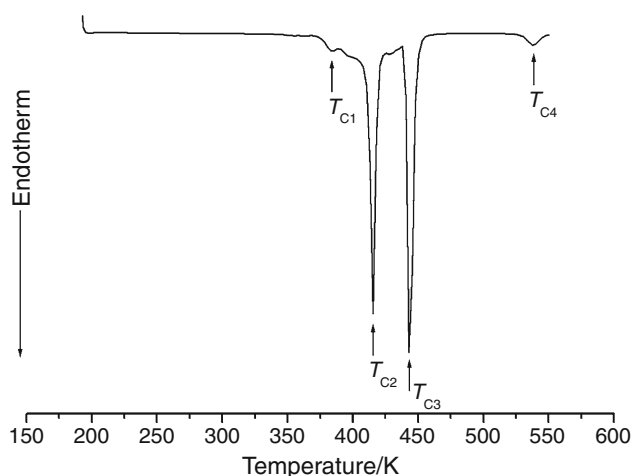


**Fig. 2** Differential scanning calorimetry (DSC) thermogram of a  $(\text{NH}_4)_2\text{Co}(\text{SO}_4)_2 \cdot 6\text{H}_2\text{O}$  single crystal

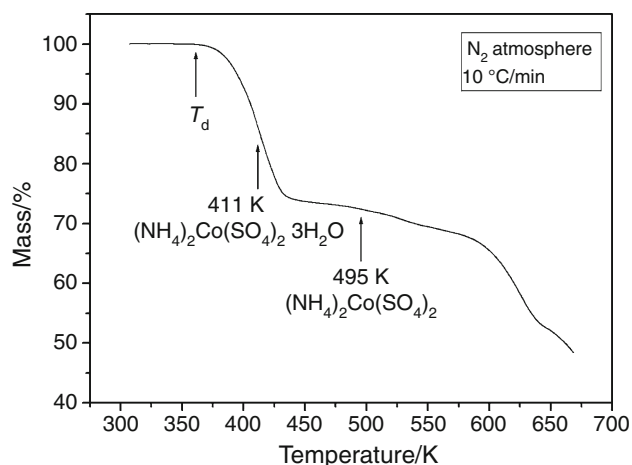


**Fig. 3** The thermogravimetry analysis (TG) of a  $(\text{NH}_4)_2\text{Co}(\text{SO}_4)_2 \cdot 6\text{H}_2\text{O}$  crystal

360 K =  $T_d$  is due to the onset of partial thermal decomposition, and that the transformation anomalies at 384 K =  $T_{C1}$ , 415 K =  $T_{C2}$ , and 443 K =  $T_{C3}$  are related to phase transitions. In addition, the endothermic peak at 518 K is due to melting.

The NMR spectrum for the  $^1\text{H}$  nuclei in a  $(\text{NH}_4)_2\text{Co}(\text{SO}_4)_2 \cdot 6\text{H}_2\text{O}$  crystal was measured for various temperatures. There are two kinds of protons in  $(\text{NH}_4)_2\text{Co}(\text{SO}_4)_2 \cdot 6\text{H}_2\text{O}$ : the “ammonium” protons for which relaxation is mainly determined by the hindered rotation of the  $\text{NH}_4$  groups, and the “hydrogen bond” protons for which relaxation is mainly determined by the motion of the hydrogens in hydrogen sulfate ions. In our results, the proton signals due to the ammonium and hydrogen bond protons overlap, and the line width due to the ammonium and hydrogen bond protons is very broad. Therefore, we

cannot distinguish the ammonium and hydrogen bond protons.

The temperature dependence of the paramagnetic shift of the  $^1\text{H}$  signal of a  $(\text{NH}_4)_2\text{Co}(\text{SO}_4)_2 \cdot 6\text{H}_2\text{O}$  crystal with respect to a reference signal is presented in Fig. 4. In general, the paramagnetic shift is sensitive to the electric environment of the nucleus. The paramagnetic shift near  $T_{C1}$  is more or less continuous. Near  $T_{C2}$ , the paramagnetic shift abruptly changes with increasing temperature, which is due to the phase transition. The shift in the resonance lines of  $(\text{NH}_4)_2\text{Co}(\text{SO}_4)_2 \cdot 6\text{H}_2\text{O}$  might be due to the dipole–dipole interactions between the magnetic moments of the  $\text{NH}_4^+$  nuclei and the magnetic moments of the  $\text{Co}^{2+}$  atoms. The relative intensity of the  $^1\text{H}$  signal is shown as a function of temperature in the inset in Fig. 4. As the temperature is increased, the intensity of the signal decreases and becomes quite weak above  $T_{C2} = 415$  K, which indicates that the protons play an important role in this phase transition. We conclude that the decrease in the intensity of the signal with temperature is related to the loss of  $\text{H}_2\text{O}$ .

The  $^1\text{H}$  spin–lattice relaxation time,  $T_1$ , was obtained for  $(\text{NH}_4)_2\text{Co}(\text{SO}_4)_2 \cdot 6\text{H}_2\text{O}$  at a frequency of 200 MHz. The saturation recovery traces of the magnetizations of  $^1\text{H}$  at several different temperatures were measured. The measured magnetization recoveries were found to be satisfactorily fitted with the single exponential function,  $[S(\infty) - S(t)]/S(\infty) = \exp(-Wt)$ , where  $S(t)$  is the nuclear magnetization at time  $t$  and  $W$  is the transition probability corresponding to  $\Delta m = \pm 1$ . The relaxation rate is given by  $1/T_1 = W$  [28]. The spin–lattice relaxation recoveries at 200, 300, and 400 K are shown in Fig. 5. Although the early parts of the decay lines in Fig. 5 do not intersect with the y-axis at one due to imperfect saturation pulses, the spin–lattice relaxation recovery is a single exponential

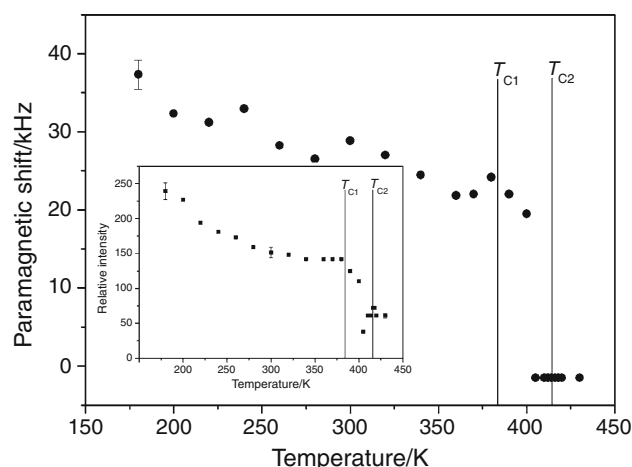


**Fig. 4** The paramagnetic shift of the  $^1\text{H}$  signal as a function of temperature (inset the temperature dependence of the relative intensity of the  $^1\text{H}$  signal)

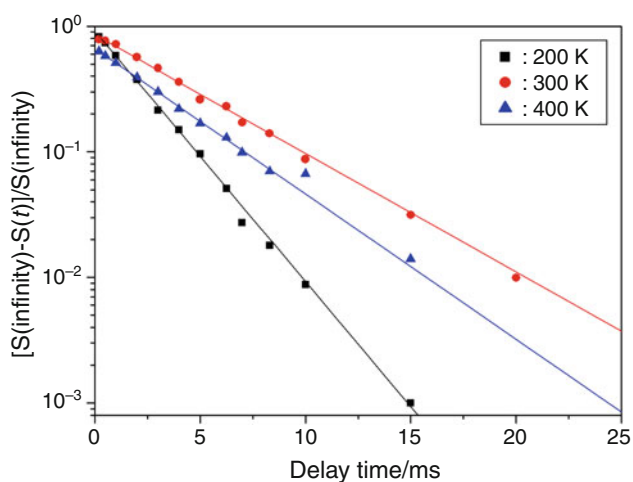


**Fig. 5** The saturation recovery traces of  $^1\text{H}$  as functions of the delay time (filled square 200 K, filled circle 300 K, and filled triangle 400 K)

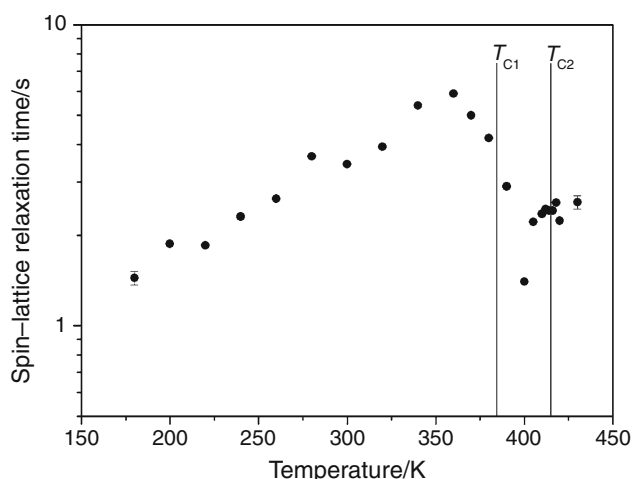


**Fig. 6** The temperature dependence of the spin–lattice relaxation time,  $T_1$ , for the  $^1\text{H}$  nuclei in a  $(\text{NH}_4)_2\text{Co}(\text{SO}_4)_2 \cdot 6\text{H}_2\text{O}$  single crystal

decay at all temperatures. The slopes of the recovery traces at each temperature are different. This figure shows the vast variation in the proton dynamics of the hydrogen bond networks associated with the successive phase transitions.

The  $^1\text{H}$  relaxation time was obtained in terms of  $W$ , and the spin–lattice relaxation time,  $T_1$ , was found to have a very strong temperature dependence, as shown in Fig. 6. The relaxation time for the  $^1\text{H}$  nuclei passes through a maximum value near  $T_d$ . This temperature is related to the beginning of the loss of  $\text{H}_2\text{O}$ , as observed in the TG results. There is an abrupt drop in  $T_1$  near  $T_{C1} = 384$  K, and the change in the temperature dependence of  $T_1$  near  $T_{C2} = 415$  K is related to the loss of  $\text{H}_2\text{O}$ ; the forms of the octahedra of water molecules surrounding  $\text{Co}^{2+}$  are probably disrupted by the loss of  $\text{H}_2\text{O}$ . Further, the spin–lattice

relaxation time of the  $^1\text{H}$  nuclei is very long. Here, one of the N–H bonds of an  $\text{NH}_4^+$  ion is parallel to the crystallographic  $c$ -axis, which was parallel to the external magnetic field for the  $T_1$  measurements. Therefore,  $T_1$  for the uniaxial rotation of the  $\text{NH}_4^+$  ion around an axis parallel to the crystallographic  $c$ -axis is very long, since the angle made by the H–H vector and the external magnetic field is not changed by this rotational mode.

## Conclusions

The thermodynamic properties of  $(\text{NH}_4)_2\text{Co}(\text{SO}_4)_2 \cdot 6\text{H}_2\text{O}$  single crystals were investigated and phase transitions were found at 384, 415, and 443 K. This crystal undergoes the loss of  $\text{H}_2\text{O}$  with increasing temperature. The first mass loss in  $(\text{NH}_4)_2\text{Co}(\text{SO}_4)_2 \cdot 6\text{H}_2\text{O}$  occurs in the vicinity of 360 K ( $T_d$ ), which is interpreted as the onset of partial thermal decomposition. The changes in the temperature dependence of  $T_1$  at  $T_{C1}$  and  $T_{C2}$  are associated with the structural phase transitions of this crystal. The  $\text{NH}_4^+$  ions are surrounded by one water and five  $\text{SO}_4$  oxygens and play important roles in this phase transition, which is associated with slight rotations of the  $\text{SO}_4$  tetrahedra, a slight distortion of the lattice, and the proton hopping or breaking of hydrogen bonds in the neighborhood of the  $\text{NH}_4^+$  ions. These mechanisms at high temperatures are related to hydrogen bond proton transfer involving the breakage of a weak hydrogen bond and the formation of a new hydrogen bond.

**Acknowledgements** This study was supported by the Mid-Career Researcher Program through an NRF grant funded by the MEST (No. 2011-0000107).

## References

- Jain VK, Venkateswarlu P. On the  $^{57}\text{Fe}$  Mossbauer spectra of  $\text{FeTe}$  and  $\text{Fe}_2\text{Te}_3$ . *J Phys C Solid State Phys.* 1979;12:865–73.
- Gronvold F, Meisingset KK. Thermodynamic properties and phase transitions of salt hydrates between 270 and 400 K I.  $\text{NH}_4\text{Al}(\text{SO}_4)_2 \cdot 12\text{H}_2\text{O}$ ,  $\text{KAl}(\text{SO}_4)_2 \cdot 12\text{H}_2\text{O}$ ,  $\text{Al}_2(\text{SO}_4)_3 \cdot 17\text{H}_2\text{O}$ ,  $\text{ZnSO}_4 \cdot 7\text{H}_2\text{O}$ ,  $\text{Na}_2\text{SO}_4 \cdot 10\text{H}_2\text{O}$ , and  $\text{Na}_2\text{S}_2\text{O}_3 \cdot 5\text{H}_2\text{O}$ . *J Chem Therm.* 1982;14:1083–98.
- Lim AR, Lee JH.  $^{23}\text{Na}$  and  $^{87}\text{Rb}$  relaxation study of the structural phase transitions in the Tutton salts  $\text{Na}_2\text{Zn}(\text{SO}_4)_2 \cdot 6\text{H}_2\text{O}$  and  $\text{Rb}_2\text{Zn}(\text{SO}_4)_2 \cdot 6\text{H}_2\text{O}$  single crystals. *Phys Status Solidif B.* 2010;247:1242–6.
- Montgomery H, Lingafelter EC. The crystal structure of Tutton's salts, III. Copper ammonium sulfate hexahydrate. *Acta Crystallogr.* 1966;20:659–62.
- Brown GM, Chidambaram R. The structure of copper ammonium sulfate hexahydrate from neutron diffraction data. *Acta Crystallogr. B.* 1969;25:676–87.
- Marinova D, Georgiev M, Stoilova D. Vibrational behavior of matrix-isolated ions in Tutton compounds. II. Infrared

- spectroscopic study of  $\text{NH}_4^+$  and  $\text{SO}_4^{2-}$  ions included in copper sulfates and selenates. *J Mol Struct.* 2009;938:179–84.
7. Marinova D, Georgiev M, Stoilova D. Vibrational behavior of matrix- isolated ions in Tutton compounds. I. Infrared spectroscopic study of  $\text{NH}_4^+$  and  $\text{SO}_4^{2-}$  ions included in magnesium sulfates and selenates. *J Mol Struct.* 2009;929:67–72.
  8. Marinova D, Georgiev M, Stoilova D. Vibrational behavior of matrix- isolated ions in Tutton compounds. IV. Infrared spectroscopic study of  $\text{NH}_4^+$  and  $\text{SO}_4^{2-}$  ions included in nickel sulfates and selenates. *Cryst Res Technol.* 2010;45:637–42.
  9. Georgiev M, Marinova D, Stoilova D. Vibrational behavior of matrix- isolated ions in Tutton compounds. III. Infrared spectroscopic study of  $\text{NH}_4^+$  and  $\text{SO}_4^{2-}$  ions included in cobalt sulfates and selenates. *Vib Spectrosc.* 2010;53:233–8.
  10. Anandalakshmi H, Parthiban S, Parvathi V, Thanikachalam V, Mojumdar SC. Thermal and optical properties of Cu(II)-doped magnesium rubidium sulfate hexahydrate crystals. *J Therm Anal Calorim.* 2011;104:963–7.
  11. Parthiban S, Murali S, Madhurambal G, Meenakshisundaram SP, Mojumdar SC. Effect of zinc(II) doping on thermal and optical properties of potassium hydrogen phthalate (KHP) crystals. *J Therm Anal Calorim.* 2010;100:751–6.
  12. Misra SK, Sun JS. EPR of a  $\text{VO}_2^+$  doped  $\text{Zn}(\text{NH}_4)_2(\text{SO}_4)_2 \cdot 6\text{H}_2\text{O}$  single crystal: Ligand superhyperfine interaction. *Phys Rev B.* 1990;42:8601–4.
  13. Misra SK, Sun JS. EPR of  $\text{VO}_2^+$  in  $\text{Cd}(\text{NH}_4)_2(\text{SO}_4)_2 \cdot 6\text{H}_2\text{O}$  and  $\text{Mg}(\text{NH}_4)_2(\text{SO}_4)_2 \cdot 6\text{H}_2\text{O}$  single crystals. Ligand superhyperfine interaction and bonding coefficients. *Physica B.* 1990;162:331–43.
  14. Misra SK, Sun JS, Li X. EPR and optical absorption studies of a  $\text{VO}_2^+$  doped  $\text{Co}(\text{NH}_4)_2(\text{SO}_4)_2 \cdot 6\text{H}_2\text{O}$ . *Physica B.* 1991;168:170–6.
  15. Jain VK, Kapoor V, Prakash V. Electron paramagnetic resonance of  $\text{Mn}^{2+}$  in  $\text{Cs}_2\text{M}(\text{SO}_4)_2 \cdot 6\text{H}_2\text{O}$  ( $\text{M} = \text{Mg}, \text{Zn}, \text{Co}, \text{Ni}$ ) single crystals. *Solid State Commun.* 1996;97:425–8.
  16. Hoffmann SK, Augustyniak MA, Goslar J, Hilczer W. Does the Jahn-Teller effect influence electron spin relaxation? Electron paramagnetic resonance and electron spin echo studies of the  $\text{Mn}^{2+}$  doped  $(\text{NH}_4)_2\text{Mg}(\text{SO}_4)_2 \cdot 6\text{H}_2\text{O}$  single crystal and comparison with  $\text{Cu}^{2+}$  data. *Mol Phys.* 1998;95:1265–73.
  17. Hoffmann SK, Kaszynski R, Augustyniak MA, Hilczer W. Restricted validity of the two state model describing a vibronic EPR  $g$ -factors averaging in  $\text{Cs}_2\text{Zn}(\text{SO}_4)_2 \cdot 6\text{H}_2\text{O}$  tutton salt crystals doped with  $\text{Cu}^{2+}$  ions. *Acta Phys Pol A.* 1999;96:733–40.
  18. Augustyniak MA, Usachev AE. The host lattice influence on the Jahn-Teller effect of the  $\text{Cu}(\text{H}_2\text{O})_6^{2+}$  complex studied by EPR in  $\text{K}_2\text{Zn}(\text{SO}_4)_2 \cdot 6\text{H}_2\text{O}$  and  $(\text{NH}_4)_2\text{Zn}(\text{SO}_4)_2 \cdot 6\text{H}_2\text{O}$  tutton salt crystals. *J Phys Condens. Matter.* 1999;11:4391–400.
  19. Hoffmann SK, Hilczer W, Goslar J, Augustyniak-Jablokow MA. Raman spin lattice relaxation, Debye temperature and disorder effects studied with electron spin echo of  $\text{Cu}^{2+}$  in Tutton salt crystals. *J Phys Condens Matter.* 2001;13:7443–57.
  20. Hoffmann SK, Goslar J, Hilczer W, Augustyniak-Jablokow MA. Electron spin relaxation of vibronic  $\text{Cu}(\text{H}_2\text{O})_6$  complexes in  $\text{K}_2\text{Zn}(\text{SO}_4)_2 \cdot 6\text{H}_2\text{O}$  single crystals. *J Phys Condens Matter.* 2001;13:707–18.
  21. Hoffmann SK, Goslar J, Hilczer W, Kaszynski R, Augustyniak-Jablokow MA. Electron spin relaxation of the Jahn-Teller  $\text{Cu}(\text{H}_2\text{O})_6$  complex in  $\text{Cs}_2\text{Zn}(\text{SO}_4)_2 \cdot 6\text{H}_2\text{O}$  crystal. *Solid State Commun.* 2001;117:333–6.
  22. Ravi S, Subramanian P. Electron paramagnetic resonance study of  $\text{Cr}^{3+}$  ions in  $(\text{NH}_4)_2\text{Co}(\text{SO}_4)_2 \cdot 6\text{H}_2\text{O}$  single crystal. *Solid State Commun.* 2006;138:129–31.
  23. Ravi S, Subramanian P. Raman spin-lattice relaxation time and Debye temperature studies of  $\text{Cr}^{3+}$  in ammonium cobalt sulphate hexahydrate single crystal. *J Phys Chem Solid.* 2007;68:1549–51.
  24. Ravi S, Subramanian P. Theoretical explanation of EPR parameters for  $\text{Cr}^{3+}$  in  $(\text{NH}_4)_2\text{Co}(\text{SO}_4)_2$  crystal. *Physica B.* 2007;393:275–7.
  25. Riley MJ, Hitchman MA, Mohammed AW. Interpretation of the temperature dependent  $g$  values of the  $\text{Cu}(\text{H}_2\text{O})_6^{2+}$  ion in several host lattices using a dynamic vibronic coupling model. *J Chem Phys.* 1987;87:3766–78.
  26. Hoffmann SK, Goslar J, Hilczer W, Augustyniak MA, Marciniak M. Vibronic behavior and electron spin relaxation of Jahn-Teller complex  $\text{Cu}(\text{H}_2\text{O})_6^{2+}$  in  $(\text{NH}_4)_2\text{Mg}(\text{SO}_4)_2 \cdot 6\text{H}_2\text{O}$  single crystal. *J Phys Chem A.* 1998;102:1697–707.
  27. Montgomery F, Lingafelter EC. The crystal structure of Tutton's salts. VI. Vanadium(II), iron(II) and cobalt (II) ammonium sulfate hexahydrates. *Acta Crystallogr.* 1962;22:775–80.
  28. Lim AR, Shin HK.  $^1\text{H}$  and  $^7\text{Li}$  nuclear magnetic resonance study of the superionic crystals  $\text{K}_4\text{LiH}_3(\text{SO}_4)_4$  and  $(\text{NH}_4)_4\text{LiH}_3(\text{SO}_4)_4$ . *J Appl Phys.* 2010;107:63513–8.